Anti-function solution of uniaxial anisotropic Stoner-Wohlfarth model

Kun Zheng(郑坤), Yu Miao(缪宇), Tong Li(李通), Shuang-Long Yang(杨双龙), Li Xi(席力), Yang Yang(杨洋), Dun Zhao(赵敦), and De-Sheng Xue(薛德胜)

Citation: Chin. Phys. B, 2022, 31 (**4**): 040202. DOI: 10.1088/1674-1056/ac401e
Journal homepage: http://cpb.iphy.ac.cn; http://iopscience.iop.org/cpb

What follows is a list of articles you may be interested in

Ultra-broadband absorber based on cascaded nanodisk arrays

Qi Wang(王琦), Rui Li(李瑞), Xu-Feng Gao(高旭峰), Shi-Jie Zhang(张世杰), Rui-Jin Hong(洪瑞金), Bang-Lian Xu(徐邦联), and Da-Wei Zhang(张大伟)

Chin. Phys. B, 2022, 31 (**4**): 040203. DOI: 10.1088/1674-1056/ac2d1d

A new algorithm for reconstructing the three-dimensional flow field of the oceanic mesoscale eddy

Chao Yan(颜超), Jing Feng(冯径), Ping-Lv Yang(杨平吕), and Si-Xun Huang(黄思训)

Chin. Phys. B, 2021, 30 (**12**): 120204. DOI: 10.1088/1674-1056/ac29af

Novel energy dissipative method on the adaptive spatial discretization for the Allen-Cahn equation

Jing-Wei Sun(孙竟巍), Xu Qian(钱旭), Hong Zhang(张弘), and Song-He Song(宋松和)

Chin. Phys. B, 2021, 30 (**7**): 070201. DOI: 10.1088/1674-1056/abe37b

Constructing reduced model for complex physical systems via interpolation and neural networks

Xuefang Lai(赖学方), Xiaolong Wang(王晓龙, and Yufeng Nie(聂玉峰)

Chin. Phys. B, 2021, 30 (**3**): 030204. DOI: 10.1088/1674-1056/abd92e

A meshless algorithm with the improved moving least square approximation for nonlinear improved Boussinesq equation

Yu Tan(谭渝) and Xiao-Lin Li(李小林)

Chin. Phys. B, 2021, 30 (**1**): 010201. DOI: 10.1088/1674-1056/abaed7

Anti-function solution of uniaxial anisotropic Stoner–Wohlfarth model

Kun Zheng(郑坤)[1], Yu Miao(缪宇)[1], Tong Li(李通)[1], Shuang-Long Yang(杨双龙)[1], Li Xi(席力)[1], Yang Yang(杨洋)[1], Dun Zhao(赵敦)[2,†], and De-Sheng Xue(薛德胜)[1,‡]

[1] *Key Laboratory for Magnetism and Magnetic Materials of the Ministry of Education, Lanzhou University, Lanzhou* 730000, *China*
[2] *School of Mathematics and Statistics, Lanzhou University, Lanzhou* 730000, *China*

(Received 29 July 2021; revised manuscript received 16 November 2021; accepted manuscript online 5 December 2021)

The anti-trigonometric function is used to strictly solve the uniaxial anisotropic Stoner–Wohlfarth (SW) model, which can obtain the relation of the angle $\alpha(\theta)$ between the magnetization (the anisotropy field) and the applied magnetic field. Using this analytic solution, the hysteresis loops of uniaxial anisotropic SW particles magnetized in typical directions could be numerically calculated. Then, the hysteresis loops are obtained in randomly distributed SW particle ensembles while ignoring the dipole interaction among them with the analytic solution. Finally, the correctness of the analytic solution is verified by the exact solutions of remanence, switching field, and coercivity from the SW model. The analytic solution provides an important reference for understanding the magnetizing and magnetization reversal processes of magnetic materials.

Keywords: Stoner–Wohlfarth model, anti-trigonometric function, hysteresis loop

PACS: 02.60.Cb, 75.30.Gw, 75.40.Cx, 75.60.Ej **DOI:** 10.1088/1674-1056/ac401e

1. Introduction

There are three major magnetizing and magnetization reversal mechanisms in magnetic materials: coherent rotation,[1] domain wall motion,[2] and nucleation.[3] The Stoner–Wohlfarth (SW) model was presented and published by Stoner and Wohlfarth in the 1940s, which successfully described the coherent rotation of uniaxial anisotropic single-domain particles and predicted the switching field of non-interacting single-domain particles ensembles.[1,4] At present, the SW model is not only widely used in magnetic recording media[5–8] and hard magnets[9,10] but also a basic model for describing the dynamic magnetic properties of soft magnetic materials under microwaves.[11–15] In addition, it provides an effective analysis model for magnetoelectric transport such as anisotropic magnetoresistance and anomalous Hall effect,[16–18] and spintronics research such as spin Hall magnetoresistance and spin Hall effect.[19,20] Determining the stable direction of magnetization under an applied magnetic field is the key to obtain the magnetizing curves and hysteresis loops, as well as understand the basic magnetic physical quantities.

Figure 1 is a schematic illustration to describe the coherent rotation of the spherical Stoner–Wohlfarth (SW) particle with uniaxial anisotropy field $\boldsymbol{H}_K$ under the applied magnetic field $\boldsymbol{H}$. In the classic paper of SW, although the exact solution of the switching field magnetized in any direction was given, only the analytic solutions of the stable direction of the magnetization at $\theta = 0°$, $45°$, and $90°$ were obtained.[1,21] Surrounding the switching field, Slonczewski proposed a geometric solution of the uniaxial case in 1956, which became known as the asteroid method.[22] Thiaville extended this method to two-dimensional and three-dimensional systems under arbitrary anisotropy energy, and applied it to nano-magnetic particles.[23] On this basis, Pfeiffer discussed the influence of thermal fluctuations on magnetization jumping over the energy barriers.[24] Szabo discussed the change of the switching field in a rotational magnetic field with linear excitation.[25] Henry gave the distortion of the SW astroid in a spin-polarized current.[26] Meanwhile, the remanence and coercivity have also been studied in the SW model.[27] However, there is no simple form of stable solution for the magnetization magnetized in arbitrary directions. Although it can be transformed into a 4th-order equation,[28,29] due to the non-uniqueness of the solution, it is difficult to obtain the magnetizing curves and hysteresis loops.

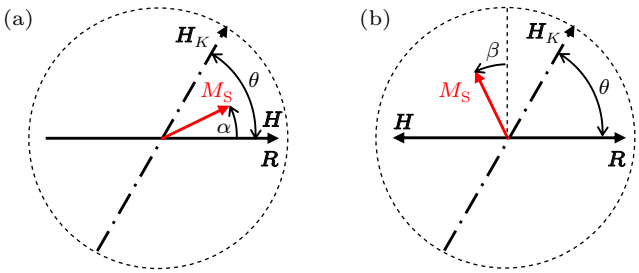

Fig. 1. Schematic illustration of SW particle. (a) The applied magnetic field $\boldsymbol{H}$ is parallel to the reference axis $\boldsymbol{R}$ in the magnetizing process, (b) the magnetization reversal process where $\boldsymbol{H}$ is antiparallel to the reference axis $\boldsymbol{R}$.

This paper directly shows the analytic solution of θ (the

†Corresponding author. E-mail: zhaod@lzu.edu.cn
‡Corresponding author. E-mail: xueds@lzu.edu.cn

angle between the anisotropy field $\boldsymbol{H}_K$ and the reference axis $\boldsymbol{R}$) varying with α (the angles between the saturation magnetization $\boldsymbol{M}_S$ and the reference axis $\boldsymbol{R}$) by using the anti-trigonometric function. Due to the anti-trigonometric function $y = f(x)$ is symmetric about $y = x$, the relation of $\alpha \sim \theta$ at different applied magnetic fields is also exposed. Then, the hysteresis loops magnetized in any direction are obtained by using $M = M_S \cos\alpha$. Using these loops, the hysteresis loops are obtained in the randomly oriented and non-interacting SW particle ensembles. Finally, the correctness of the analytic solution is verified by fitting the exact solutions of remanence, switching field and coercivity.

2. Anisotropy free energy density

The spherical SW particle is shown in Fig. 1. The total free energy density F including Zeeman energy and anisotropy energy. For the magnetizing and magnetization reversal processes, F can be expressed as

$$F(\alpha) = -\frac{K}{2}\cos 2(\theta-\alpha) - \mu_0 M_S H\cos\alpha, \tag{1a}$$

$$F(\beta) = -\frac{K}{2}\cos 2\left[\left(\frac{\pi}{2}-\theta\right)+\beta\right] - \mu_0 M_S H\cos\left(\frac{\pi}{2}-\beta\right), \tag{1b}$$

where K is the anisotropy constant, μ_0 is the vacuum permeability, M_S is the saturation magnetization, and H is the applied magnetic field. θ is the angle between the anisotropy field $\boldsymbol{H}_K$ and the reference axis $\boldsymbol{R}$, and α (β) is the angle between the saturation magnetization $\boldsymbol{M}_S$ and the reference axis $\boldsymbol{R}$ (the perpendicular direction of the reference). The stable direction of saturation magnetization can be determined by the minimum of the free energy density

$$\frac{\partial F(\alpha)}{\partial\alpha} = -\left[\sin 2(\theta-\alpha) - 2h\sin\alpha\right] = 0, \tag{2a}$$

$$\frac{\partial^2 F(\alpha)}{\partial\alpha^2} = 2\left[\cos 2(\theta-\alpha) + h\cos\alpha\right] > 0, \tag{2b}$$

$$\frac{\partial F(\beta)}{\partial\beta} = \left[\sin 2(\theta-\beta) - 2h\cos\beta\right] = 0, \tag{3a}$$

$$\frac{\partial^2 F(\beta)}{\partial\beta^2} = -2\left[\cos 2(\theta-\beta) - h\sin\beta\right] > 0, \tag{3b}$$

where $h = H/H_K$ is the reduced field and $H_K = 2K/\mu_0 M_S$ is the anisotropy field.

3. The anti-trigonometric solution of $\alpha \sim \theta$

It can be directly obtained from Eqs. (2a) and (3a)

$$\theta(\alpha) = \alpha + \frac{1}{2}\arcsin(2h\sin\alpha), \tag{4a}$$

$$\theta(\beta) = \beta + \frac{1}{2}\arcsin(2h\cos\beta). \tag{4b}$$

Let $\theta(\alpha) = f(\alpha)$ and $\theta(\beta) = g(\beta)$. The anti-trigonometric solution of α can be directly obtained from Eqs. (4a) and (4b)

$$\alpha = f^{-1}(\theta), \tag{5a}$$

$$\alpha = \frac{\pi}{2} - \beta = \frac{\pi}{2} - g^{-1}(\theta). \tag{5b}$$

The former and latter reflect the solution of the magnetizing and magnetization reversal processes, respectively. Determining all possible stable solutions in Eqs. (4a) and (4b) are the key to obtain the magnetizing curves and hysteresis loops using Eqs. (5a) and (5b).

It is known that the domain of the $y = \arcsin(x)$ is $[-1,1]$, and the range is $[-\pi/2,\pi/2]$.[30] It can be seen that the domain of Eqs. (4a) and (4b) satisfies $-1 \le 2h\sin\alpha \le 1$ and $-1 \le 2h\cos\beta \le 1$, respectively. Then their ranges are $-\pi/4 \le (\theta-\alpha) \le \pi/4$ and $-\pi/4 \le (\theta-\beta) \le \pi/4$. Because $(\theta-\alpha)$ is the angle between the saturation magnetization and the anisotropy field, we can obtain the solution in $-\pi/4 \le (\theta-\alpha) \le \pi/4$ by Eq. (4a), as shown in the grey area I of Fig. 2. Considering $\beta = \alpha - \pi/2$, we can obtain the solution in $-3\pi/4 \le (\theta-\alpha) \le -\pi/4$ by Eq. (4b), as shown in the yellow area I of Fig. 2. If we consider another direction of the anisotropy field where the magnetization deviates from the easy axis, Eqs. (4a) and (4b) can describe the gray and yellow areas II in Fig. 2, respectively. Therefore, Eqs. (4a) and (4b) completely describe the magnetization deviating from the easy axis in the SW model under the applied magnetic field in the entire space.

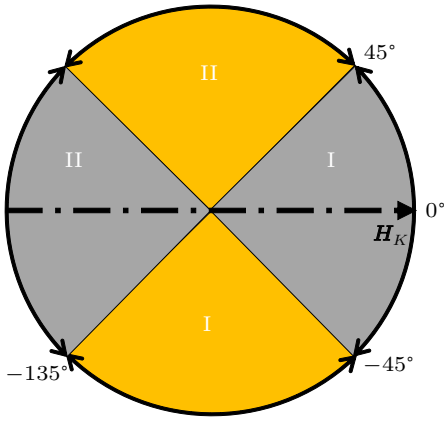

Fig. 2. The solution of Eqs. (4a) and (4b). I and II represent the results of the magnetization deviating from the anisotropy field H_K and $-H_K$, respectively. The gray and yellow areas represent the results of magnetizing and magnetization reversal, respectively.

The relation curve of $\theta \sim \alpha$ can be obtained by Eqs. (4a) and (4b), as shown in Fig. 3(a). The solid line and the dotted line respectively represent the $\theta = f(\alpha)$ and $\theta = g(\beta)$, when θ is limited in $[0,\pi/2]$. As the reduced field h changing in $[-\infty,-1]$ and $[-0.5,\infty]$, the solutions of Eqs. (4a) and (4b) show a continuous curve of $\theta \sim \alpha$. Moreover, it is not a continuous curve of $\theta \sim \alpha$ when h changes in $(-1,-0.5)$,

as shown by the curve of $h = -0.6$ and -0.75 in Fig. 3(a). It is because that the magnetization will jump when h changes in $(-1, -0.5)$.[22,23] The position (α, θ) of the horizontal tangent of the curve corresponds to the unstable position under the switching field $h_{\rm SW}$. According to the definition of the anti-trigonometric function,[30] the function $\alpha = f^{-1}(\theta)$ can be obtained by symmetrically transforming $\theta = f(\alpha)$ with a straight line $\theta = \alpha$. This result can be used to obtain the stable magnetization angle α when the applied magnetic field changes under a given applied field angle θ.

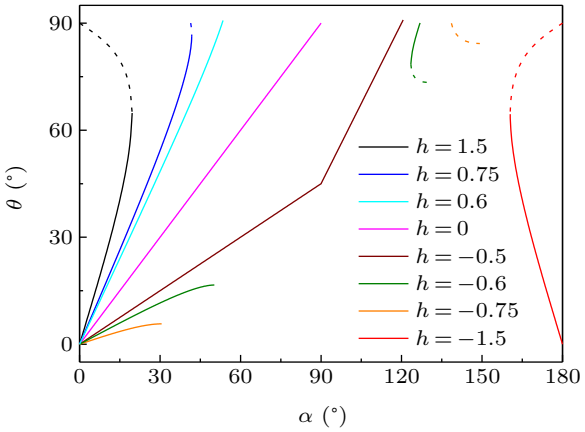

Fig. 3. The relation curve of $\theta \sim \alpha$ with different reduced fields h as 1.5, 0.75, 0.6, 0, -0.5, -0.6, -0.75, and -1.5, respectively. The solid line and the dotted line are the solutions of Eqs. (4a) and (4b), respectively.

4. Hysteresis loops

Let the direction of reference axis $\boldsymbol{R}$ be the initial direction of $\boldsymbol{H}$. The hysteresis loop is the projection of the magnetization in the reference axis direction. In a uniaxial system, when $\boldsymbol{H}$ changes, the deviation of the magnetization from the easy axis involves two anisotropy field directions. If the angles between $\boldsymbol{H}$ and the two anisotropy fields are the same, the angle of the magnetization deviating from the easy axis is equal. Therefore, we only need to deal with one case where the magnetization deviates from an anisotropy field. Another case can be described in the hysteresis loop through an inversion center of the previous result.

For the first case, the relation curve of $\cos\alpha \sim \theta$ under different reduced fields h in the reference direction $\boldsymbol{R}$ can be obtained by using the function $\alpha = f^{-1}(\theta)$, as shown in Fig. 4(a). For any given applied field angle θ, $\cos\alpha = M/M_{\rm S}$ under different reduced fields h is obtained on the $\cos\alpha \sim \theta$ curve in the order of reduced field h from large to small and from positive to negative. Then we plot the points of $(h, M/M_{\rm S})$ in sequence to get the magnetizing and magnetization reversal curves. Figure 4(b) shows the relation curve of $M/M_{\rm S} \sim h$ at $\theta = 16.6°$ and $73.4°$. To demonstrate this idea, we take $\theta = 73.4°$ as an example to illustrate the specific process. The points A, B, $C_{1,2}$, and D correspond to the points $(h, M/M_{\rm S})$ under $h = 1.5$, 0, -0.6, and -0.5 in Figs. 4(a) and 4(b). C_1 and C_2 are the points before and after the magnetization jump under the switching field $h_{\rm SW} = -0.6$. Then, in the coordinate system with $M/M_{\rm S}$ as the vertical axis and h as the horizontal axis. We can draw points from A, and then draw the remaining $(h, M/M_{\rm S})$ points in descending order of the reduced field h, including the remanence B under $h = 0$ and C_1 and C_2 under switching field $h_{\rm SW} = -0.6$. Finally, we draw to D. Connect all the points into a line to get the magnetizing and magnetization reversal curves of the first case, as shown in the red solid line of Fig. 4(b). The red dotted line in Fig. 4(b) is the center inversion of the first case. It is worth noticing that there is no saturation magnetization in the magnetic moment at other applied field angles, except for $\theta = 0°$ and $90°$. This model can also be used to judge the stable magnetization position and saturation magnetization in the measurement of soft magnetic high-frequency[11] and magnetoelectric transport.[17]

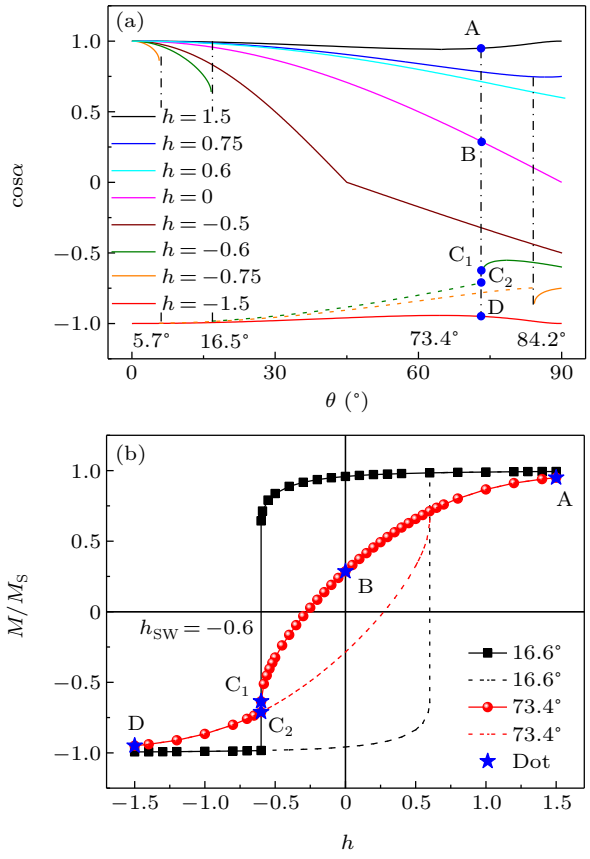

Fig. 4. (a) The relation curve of $\cos\alpha \sim \theta$ with different reduced fields h as 1.5, 0.75, 0.6, 0, -0.5, -0.6, -0.75, and -1.5. The dotted line is the relation curve of $\cos\alpha \sim \theta$ after the magnetization jumps under $h_{\rm SW}$, which is equal to the relation curve of $-\cos\alpha \sim \theta$ under $-h_{\rm SW}$. (b) The hysteresis loop at $\theta = 16.6°$ and $73.4°$. The points A, B, $C_{1,2}$ and D in panels (a) and (b) correspond to the points $(h, M/M_{\rm S})$ under $h = 1.5$, 0, -0.6, and -0.5 at $\theta = 73.4°$.

5. Randomly oriented and non-interacting SW particle ensembles

Based on the relation curve of $M/M_{\rm S} \sim \theta$, the representative hysteresis loops of the randomly oriented and non-interacting SW particle ensembles can be obtained. Because of

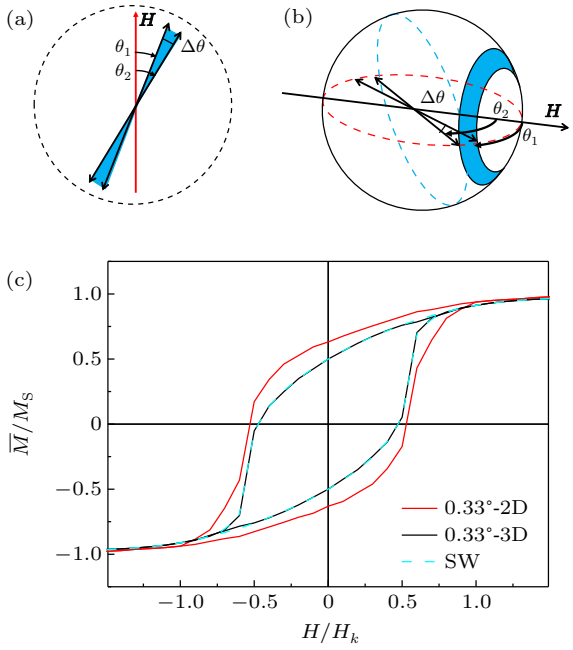

Fig. 5. (a) Schematic illustration of the SW particle ensembles in a two-dimensional (2D) plane. The distribution of SW particles at different angles θ is uniform. (b) The SW particles are not uniformly distributed as the angle θ increases in three-dimensional (3D) systems. (c) The hysteresis loops of SW particle ensembles and the blue dotted line is given by Stoner and Wohlfarth in 1948.

the different distribution of SW particles in different dimensions, we use two different averaging methods to deal with. For the first case, the distribution of SW particles in all directions is equal with the increase of θ in a 2D plane. Then, we divide the central angle into n parts ($n \to \infty$) along the direction of H, and each part is $\Delta\theta$. The length of the circle is also divided into n parts, and each arc length is $\Delta L = R\Delta\theta$, as shown in Fig. 5(a). According to the symmetry of the SW model,[1] the hysteresis loop of θ in the interval $[0,\pi]$ and $[\pi,2\pi]$ is equal. Therefore, the hysteresis loops of the SW particle ensembles can be obtained in $\theta \in [0,\pi]$

$$\overline{M(h)} = \frac{\sum_i R\Delta\theta M(h)_i}{\int_0^\pi R\,\mathrm{d}\theta} = \frac{\sum_i \Delta\theta M(h)_i}{\pi}. \tag{6}$$

$M(h)_i$ is the magnetization under the reduced field h at the applied field angle θ, and $\Delta\theta$ is the adjacent angular interval. Another situation is in a 3D sphere. The associated revolution surface will be larger as the angle θ increasing in the range of $\theta \in [0,\pi/2]$, so SW particles do not have the same number in every direction. In order to solve this problem, the central angle is equally divided into n parts ($n \to \infty$). The sphere is also divided into n slices at the same time, as shown in Fig. 5(b). Then the peripheral area of a thin slice is $\Delta s = 2\pi R^2 \sin\theta\Delta\theta$ ($\theta \in [0,\pi]$), the hysteresis loops in the plane could be refined following spheroidal-based weighting[1,31]

$$\overline{M(h)} = \frac{\sum_i 2\pi R^2 \sin\theta_i \Delta\theta M(h)_i}{\int_0^\pi 2\pi R^2 \sin\theta\,\mathrm{d}\theta}$$

$$= \frac{1}{4\pi}\sum_i 2\pi \sin\theta_i \Delta\theta M(h)_i. \tag{7}$$

θ_i is the angle between $\boldsymbol{H}$ and the anisotropic field H_{ki} at position i. A total of 540 equiangular spaced ($\Delta\theta = 0.33°$) hysteresis loops of the applied field angle θ from to π can be obtained by Eqs. (6) and (7) as shown in Fig. 5(c). The red line represents the hysteresis loop of SW particle ensembles in a two-dimensional plane, and the black line is the result in a three-dimensional sphere. It completely coincides with the result given by Stoner and Wohlfarth in 1948.[1]

6. Verifying the correctness of the analytic solution

In order to verify the correctness of the above analytic solution, we fit the numerical solutions of remanence, switching field and coercivity with the exact solutions. It is known that the remanence M_r is the projection of the magnetization in the initial direction of $\boldsymbol{H}$ when $\boldsymbol{H}$ drops from the saturation magnetization to zero,[32]

$$M_r = M_S \cos\theta. \tag{8}$$

The switching field, where an irreversible jump of the magnetization direction occurs, is given by the condition $\partial F(\alpha)/\partial\alpha = \partial^2 F(\alpha)/\partial\alpha^2 = 0$, which leads to[23,24]

$$H_{SW} = H_K\left(\sin^{2/3}\theta + \cos^{2/3}\theta\right)^{-3/2}, \tag{9}$$

The coercivity of all applied angles are[1,33]

$$H_C = H_K\left(\sin^{2/3}\theta + \cos^{2/3}\theta\right)^{-3/2}, \quad 0 \le \theta \le \frac{\pi}{4},$$
$$H_C = \frac{1}{2}H_K \sin 2\theta, \quad \frac{\pi}{4} \le \theta \le \frac{\pi}{2}. \tag{10}$$

Based on the relation curve of $\cos\alpha \sim \theta$, the numerical solutions of coercivity, switching field, and remanence also can be obtained in different applied field directions, as shown in the dot of Fig. 6. Moreover, the numerical solutions can be completely fitted with Eqs. (8)–(10), as shown in Fig. 6, which verifies the correctness of the analytic solution.

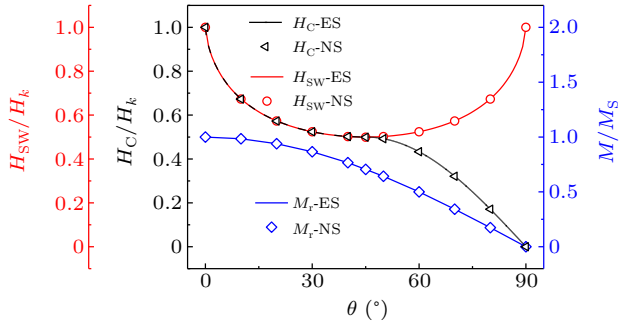

Fig. 6. The numerical (dot) and exact (line) solutions of coercivity, remanence, and switching field.

7. Conclusion

We divide the stable position where the magnetization deviates from the easy axis into two regions based on the difference between magnetizing and magnetization reversal processes and obtain the analytic solutions in the entire space by the anti-trigonometric function. Based on the relation curve of $\theta \sim \alpha$, $\cos\alpha \sim \theta$ under different reduced field h can be obtained, and then the hysteresis loops under any applied field angle can be obtained. In addition, the hysteresis loops with the easy axis of the non-interacting SW particle ensembles randomly orienting in two dimensions and three dimensions also can be obtained by the relation curve of $\cos\alpha \sim \theta$. The results of remanence, switching field, and coercivity obtained by the analytic solution are consistent with the exact solutions of the above three physical quantities. The analytic solution of the SW model is of great help to understand the actual magnetization reversal mechanism of SW particles.

Acknowledgments

Project supported by the National Natural Science Foundation of China (Grant Nos. 91963201, 12174163, and 12075102), PCSIRT (Grant No. IRT-16R35), and the 111 Project (Grant No. B20063).

References

[1] Stoner E C and Wohlfarth E P 1948 *Phil. Trans. Roy. Soc. A* **240** 599
[2] Jiles D C and Atherton D L 1986 *J. Magn. Magn. Mater.* **61** 48
[3] Kronmuller H and Durst K D 1988 *J. Magn. Magn. Mater.* **74** 291
[4] Stoner E C and Wohlfarth E P 1991 *IEEE Trans. Magn.* **27** 3475
[5] Slonczewski J C 2009 *IEEE Trans. Magn.* **45** 8
[6] Coffey K R, Thomson T and Thiele J U 2003 *J. Appl. Phys.* **93** 8471
[7] Spratt G W D, Bissel P R and Chantrell R W 1987 *IEEE Trans. Magn.* **23** 186
[8] Spratt G W D, Fearon M, Bissel P R, Chantrell R W, Lyberatos A and Wohlfarth E P 1988 *IEEE Trans. Magn.* **24** 1895
[9] Campos M F de, Romero S A, Landgraf F J G and Missell F P 2011 *J. Phys. Conf. Ser.* **303** 012049
[10] Girt E, Krishnan K M, Thomas G, Girt E and Altounian Z 2001 *J. Magn. Magn. Mater.* **231** 219
[11] Chai G Z, Xue D S, Fan X L, Li X L and Guo D W 2008 *Appl. Phys. Lett.* **93** 152516
[12] Wang C L, Zhang S H, Li S D, Du H L, Zhao G X and Cao D R 2020 *Chin. Phys. B* **29** 046202
[13] Fan X L, Xue D S, Lin M, Zhang Z M, Guo D W, Jiang C J and Wei J Q 2008 *Appl. Phys. Lett.* **92** 222505
[14] Li C Z, Jiang C J and Chai G Z 2021 *Chin. Phys. B* **30** 037502
[15] Cao X Q, Li S D, Cai Z Y, Du H L, Xue Q, Gao X Y and Xie S M 2014 *Chin. Phys. B* **23** 086201
[16] Ye J, He W, Wu Q, Liu H L, Zhang X Q, Chen Z Y and Cheng Z H 2013 *Sci. Rep.* **3** 2148
[17] Zhan Q F, Vandezande S, Haesendonck C V and Temst K 2007 *Appl. Phys. Lett.* **91** 122510
[18] Lee A J, Brangham J T, Cheng Y, White S P, Ruane W T, Esser B D, McComb D W, Hammel P C and Yang F Y 2017 *Nat. Commun.* **8** 234
[19] Li S and Zhu T 2020 *Jpn. J. Appl. Phys.* **59** 040906
[20] Shi G Y, Wan C H, Chang Y S, Li F, Zhou X J, Zhang P X, Cai J W, Han X F, Pan F and Song C 2017 *Phys. Rev. B* **95** 104435
[21] Zhong W D 1987 *Ferromagnetism*, 2nd edn. (Beijing: Science Press) pp. 329–333
[22] Slonczewski J C 1956 "Research Memorandum RM" 003.111.224, IBM Research Center Poughkeepsie, unpublished
[23] Thiaville A 1998 *J. Magn. Magn. Mater.* **182** 5
[24] Pfeiffer H 1990 *Phys. Stat. Sol.* **118** 295
[25] Szabo Z and Ivanyi A 2000 *J. Magn. Magn. Mater.* **215–216** 33
[26] Henry Y, Mangin S, Cucchiara J, Katine J A and Fullerton E E 2009 *Phys. Rev. B* **79** 214422
[27] Campos M F de, Silva F A S da, Perigo E A and Castro J A de 2013 *J. Magn. Magn. Mater.* **345** 147
[28] Wood R 2009 *IEEE Trans. Magn.* **45** 100
[29] Fal T J, Mercer J I, Leblanc M D, Whitehead J P, Plumer M L and van Ek J 2013 *Phys. Rev. B* **87** 064405
[30] He S Q 1998 *Mathematical Dictionary* (Taiyuan: Shanxi Education Press) p. 204
[31] Delgado-Garcia R, Rodriguez-Rodriguez G and Colino J M 2021 *AIP Adv.* **11** 015137
[32] Lavín R, Denardin J C, Escrig J, Altbir D, Cortés A and Gómez H 2009 *J. Appl. Phys.* **106** 103903
[33] Xue D S and Miao Y 2019 *College Physics* **38** 7